Neuron 32, 1067–1077, December 27, 2001 ©2001 Elsevier Inc. DOI 10.1016/S0896-6273(01)00548-7

Block of Kainate Receptor Desensitization Uncovers a Key Trafficking Checkpoint

Avi Priel,[1] Sanja Selak,[2] Juan Lerma,[2] and Yael Stern-Bach[1,*]
[1] The Institute of Basic Dental Sciences
The Hebrew University-Hadassah Dental School
91120 Jerusalem
Israel
[2] Instituto de Neurociencias de Alicante
CSIC-UMH
03550 San Juan de Alicante
Spain

Summary

A prominent feature of ionotropic glutamate receptors from the AMPA and kainate subtypes is their profound desensitization in response to glutamate—a process thought to protect the neuron from overexcitation. In AMPA receptors, it is well established that desensitization results from rearrangements of the interface formed between agonist-binding domains of adjacent subunits; however, it is unclear how this mechanism applies to kainate receptors. Here we show that stabilization of the binding domain dimer by the generation of intermolecular disulfide bonds apparently blocked desensitization of the kainate receptor GluR6. This result establishes a common desensitization mechanism in both AMPA and kainate receptors. Surprisingly, however, surface expression of these nondesensitizing mutants was drastically reduced and did not depend on channel activity. Therefore, in addition to its role at the synapse, we now propose an intracellular role for desensitization in controlling maturation and trafficking of glutamate receptors.

Introduction

L-glutamate, the major excitatory neurotransmitter in the brain, activates three distinct types of ionotropic glutamate receptors (iGluRs): NMDA, AMPA, and kainate, named after their relative sensitivity to agonists. All iGluRs assemble as tetramers from pools of homologous subunits. Of these, subunits GluR1-4 assemble the AMPA receptors, and subunits GluR5-7 and KA1-2 form the kainate receptors (Dingledine et al., 1999). The subunits themselves consist of four principle domains: an extracellular N-terminal domain (NTD), which is implicated in subunit oligomerization; an extracellular ligand-binding domain (LBD), composed of the so-called S1 and S2 segments; a channel-forming domain, consisting of three transmembrane domains (M1, M3, and M4) and a reentrant loop (M2); and an intracellular C-terminal domain (CTD), involved in receptor trafficking and anchoring (Madden, 2002; Mayer, 2006). Currently, structural data is available only for the LBD (Erreger et al., 2004; Mayer et al., 2006), demonstrating the special folding of S1 and S2 in two globular domains that bind glutamate in a cleft formed between them (see Figure 1C).

Activation of iGluRs is followed by either deactivation attributable to ligand unbinding or desensitization caused by closing of the ion channel pore while the receptor remains in a ligand-bound state. Both AMPA and kainate receptors desensitize completely and rapidly in response to glutamate, with a time constant of ~5 ms (Dingledine et al., 1999). This profound desensitization, together with slow recovery, is thought to play an important role in determining the frequency and amplitude of excitatory responses in the brain and may provide a backup mechanism preventing excitotoxicity during brain damage that causes an increase in glutamate concentrations at the synapse (Frandsen and Schousboe, 2003; Jones and Westbrook, 1996).

In AMPA receptors there is a strong correlation between the extent of receptor desensitization and the stability of the dimer interface formed between LBDs of adjacent subunits. Key evidence for this correlation came from a single-point mutant L-to-Y (L483Y in GluR2) that abolished desensitization (Stern-Bach et al., 1998) and was shown to stabilize the dimer interface (Sun et al., 2002). Likewise, allosteric modulators, such as cyclothiazide, bind in the interface and block AMPA receptor desensitization (Jin et al., 2005; Partin et al., 1996; Sun et al., 2002). Conversely, point mutations that weaken the interaction between neighboring LBDs greatly accelerate the desensitization (Horning and Mayer, 2004; Sun et al., 2002). These findings, together with previous work on conformational changes during ligand binding (Armstrong and Gouaux, 2000), led Sun et al. (2002) to propose the following model for receptor activation and desensitization. According to this model, glutamate binding induces LBD cleft closure, a movement that pulls apart the linkers connecting the LBD to the transmembrane domains and thus opens the channel. In the next step, the dimer interface undergoes conformational rearrangements that break the contacts between the LBDs. This uncoupling relieves the strain on the ion channel linkers, allowing the ion channel to close even though the agonist remains bound with high affinity. Despite these extensive studies on AMPA receptors, in kainate receptors a similar correlation between the stability of the dimer interface and the extent of receptor desensitization is mostly lacking. Mutations introduced to the LBD dimer interface of GluR6 only moderately attenuated the desensitization, if at all, and mostly resulted in accelerated desensitization (Fleck et al., 2003). Therefore, the role of dimer interface in kainate receptor desensitization remains an open question.

In the course of analyzing the contribution of residues in the S2 segment to GluR6 function, we found a single residue, K696, which, when mutated to arginine, present in AMPA receptors, slowed the onset of desensitization by 5-fold. Structurally, K696 projects to the dimer interface and maps close to E787 from the adjacent subunit. Mutating these sites to cysteines resulted in an apparent block of receptor desensitization. This double-cysteine

*Correspondence: yaelb@cc.huji.ac.il

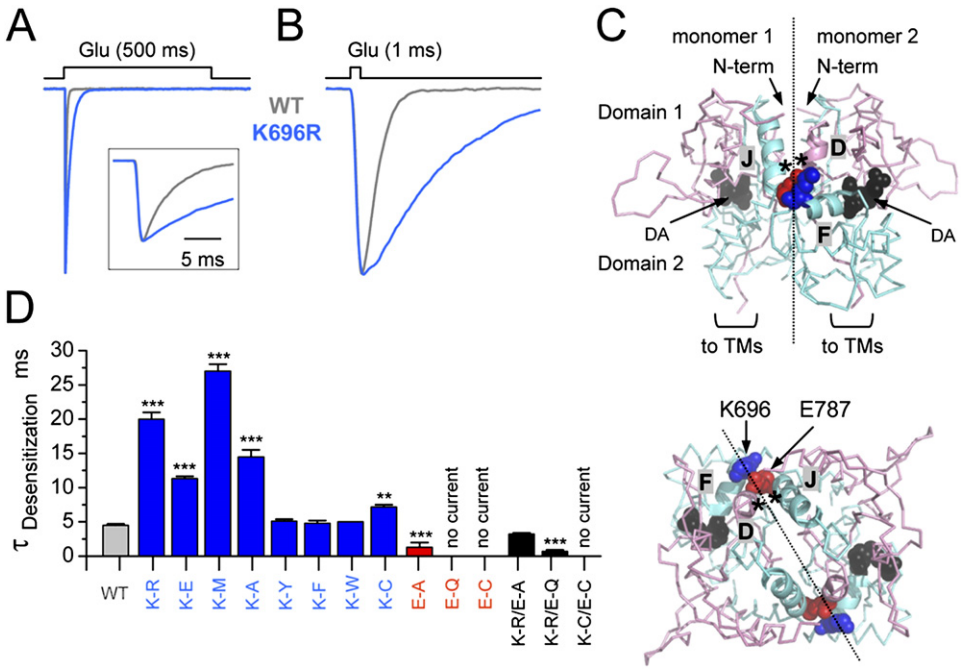

Figure 1. Interaction between Residues K696 and E787 Stabilizes the Dimer Interface of GluR6

(A and B) Superimposed normalized current traces (holding potential −60 mV) of outside-out patch recordings from HEK293 cells transiently expressing GluR6 wt (gray) and R6(K696R) (blue). Patches were exposed to 3 mM glutamate for 500 ms (A) or 1 ms (B) as indicated above the traces. Inset in (A) shows the current decay on a faster timescale.

(C) Ribbon presentation of side (upper panel) and top (lower panel) views of the GluR6 LBD dimeric structure in complex with domoic acid (PDB 1YAE; monomers b and d). In each monomer, S1 is colored pink and S2 is cyan. The dimer interface is marked by a dotted line. The relative positioning of domains 1 and 2 and the connections to the N-terminus and the transmembrane domains (TMs) are labeled. The agonist domoic acid (DA; black) and the residues K696 (blue) and E787 (red) are shown as spheres. Helixes D, F, and J are highlighted by a cartoon presentation. The position of residue Y521, which corresponds to the L-to-Y mutation in AMPA receptors, and the interacting residue L783 are marked by asterisks on helixes D and J, respectively. Figure was created by PyMOL (http://pymol.sourceforge.net).

(D) Bar plot showing the desensitization time constant (τ) of GluR6 wt (gray bar) and various point mutations at positions K696 (blue bars), E787 (red bars), or both (black bars). Bars are the mean ± SEM of 3 to 24 patches. The statistical significance (**p < 0.01, ***p < 0.001) between GluR6 wt and each mutant was determined using t test and one-way ANOVA. Mutants for which no currents could be recorded from more than 20 patches are marked by "no current."

mutation also slowed the deactivation rate and increased agonist efficacy, a phenotype resembling the behavior of the L-to-Y mutation in the AMPA receptors. These results demonstrate that the dimer interface is a pivotal participant in the mechanism of kainate receptor desensitization as well. Surprisingly, however, surface expression of this nondesensitizing mutant was drastically reduced and did not depend on channel activity. Therefore, in addition to its role at the synapse, we suggest that the desensitization state is a key checkpoint recognized by the ER quality-control machinery to ensure that only receptors that can desensitize will reach the cell surface.

Results and Discussion

Mutations at a Putative Intersubunit Pair, K696 and E787, in GluR6 Alter Receptor Kinetics

Similar to previous studies (Fleck et al., 2003; Swanson et al., 1997), we looked for subtype-specific residues that control biophysical properties of the kainate receptor GluR6. Receptors were expressed in HEK293 cells, and channel kinetics was determined using patch-clamp recordings combined with rapid solution exchange. As shown in Figure 1A, GluR6 wild-type (wt) receptors completely and rapidly desensitized in response to a prolonged application of saturating glutamate (3 mM for 500 ms) with a desensitization time constant (τdes) of 4.4 ± 0.1 ms (n = 24; Figure 1D), in agreement with published data (Dingledine et al., 1999). In the course of screening residues in the S2 segment, we found that substitution of K696, a conserved residue in GluR5/6/7, with the equivalent arginine, present in all AMPA receptor subunits, slowed the onset of GluR6 desensitization by approximately 5-fold (K696R, τdes = 20.2 ± 0.9 ms, n = 12; Figures 1A and 1D). The K696R mutation also slowed the rate of channel closure in response to a brief application of glutamate (1 ms; Figure 1B), presenting a deactivation time constant (τdea) of 9.8 ± 0.3 ms (n = 8) compared to 2.3 ± 0.3 ms (n = 7) measured for GluR6 wt receptors. In contrast to the profound effects on the desensitization and deactivation rates, the K696R mutation had no significant effect on the rate of recovery from desensitization (data not shown).

Structurally, K696, which maps to the end of helix F of the LBD (Mayer, 2005; Nanao et al., 2005), seems to project to the dimer interface and may interact with E787 from the adjacent subunit, a residue located at the end of helix J (Figure 1C). E787 is conserved across all

kainate and AMPA receptor subunits. The corresponding residue, E755, in the AMPA receptor subunit GluR2 is proposed to be part of a hydrogen-bond network that connects the base and middle of helix J of one subunit with helix D of the adjacent subunit (Horning and Mayer, 2004). We hypothesized that, in GluR6, the K696R mutation stabilizes the dimer interface by interacting with E787, thus accounting for the attenuation in receptor kinetics. Indeed, mutation of E787 to alanine (E-A), predicted to break the interaction between K696 and E787, was found to accelerate the onset of GluR6 desensitization (Figure 1D). Mutation of E787 to glutamine (E-Q) resulted in no detectable currents ($n > 20$ patches), but when combined with the K696R mutation, we observed small-current amplitudes with faster desensitization (K-R/E-Q, Figure 1D). Likewise, when combined, the K696R mutation attenuated the effect of E787A, exhibiting desensitization kinetics like GluR6 wt (K-R/E-A; Figure 1D). Based on these observations, we expected that mutation of K696 to alanine would accelerate the desensitization as observed for R6(E787A). However, instead we observed a reduced desensitization rate similar to the K696R mutation (Figure 1D). A similar reduced rate was also observed for K696 mutation to glutamate (K-E) or methionine (K-M), but not when mutated to phenylalanine (K-F), tyrosine (K-Y), or tryptophan (K-W), which exhibited GluR6 wt kinetics (Figure 1D). Although these results may not support a direct interaction between K696 and E787, the bidirectional kinetic effects of mutations at these positions support the hypothesis that the stability of the dimer interface is an important determinant of kainate receptor desensitization.

To further establish a correlation between dimer interface stability and the extent of desensitization, we attempted to generate a nondesensitizing receptor by restricting dimer movement. Due to the short distance between K696 and E787, we predicted that mutating these residues to cysteines would generate an intersubunit disulfide bond, thereby locking the dimer conformation. However, no currents could be recorded from the double-cysteine mutant R6(K696C/E787C) ($n > 50$ patches). The single-cysteine mutant R6(K696C) exhibited current amplitudes compatible to GluR6 wt, with a moderate shift of the desensitization rate (τdes = 7.2 ± 0.3 $n = 5$ $p < 0.01$; Figure 1D), while no currents could be recorded from cells expressing the R6(E787C) mutant ($n > 20$ patches).

Block of GluR6 Desensitization by the Double-Cysteine Mutation K696C/E787C Establishes a Common Desensitization Mechanism in Kainate and AMPA Receptors

In parallel to the experiments in HEK293 cells, we expressed the various mutants in *Xenopus* oocytes, and the extent of GluR6 receptor desensitization was estimated by measuring whole-cell currents before and after treatment with concanavalin A (ConA), a desensitization blocker of kainate receptors (Mayer and Vyklicky, 1989; Partin et al., 1993). As seen in Figure 2, application of glutamate for 2 s to oocytes expressing GluR6 wt receptors evoked only small currents (3–10 nA), if at all, reflecting the fast and complete desensitization of these receptors. However, after blocking the desensitization with ConA, robust steady-state currents (2–4 μA) were observed. The R6(K696R), in which the desensitization rate is ~5-fold slower (Figure 1), exhibited a brief response to glutamate, which comprised ~15% of the steady-state current recorded with ConA (Figure 2A). The single-cysteine mutant R6(K696C) behaved like GluR6 wt, while no currents could be recorded from oocytes expressing the counterpart mutant R6(E787C) even after treatment with ConA (Figure 2A). These results are similar to what we observed in the HEK293 cells. Surprisingly, however, in contrast to the apparent loss of function in the HEK293 cells, glutamate evoked high steady-state currents in oocytes expressing the double-cysteine mutant R6(K696C/E787C), which were not further affected by ConA. This result suggested that desensitization in this mutant is apparently blocked, as we initially predicted. In addition, we observed that, upon removal of glutamate, the duration of current return to baseline was 3- to 5-fold longer than that observed for GluR6 wt or for the mutants R6(K696R) and R6(K696C) (Figure 2A, note the timescale). In support of intersubunit connection between K696C and E787C in creating the nondesensitized phenotype, high steady-state currents were recorded from oocytes coexpressing the single-cysteine mutants, R6(K696C) and R6(E787C). This steady-state current comprised ~30% of the currents recorded after ConA treatment, reflecting the mixed population of desensitizing and nondesensitizing receptors. To further support the idea that the double-cysteine mutant R6(K696C/E787C) generates nondesensitizing current in the absence of ConA, we recorded excised patches from oocytes and subjected them to fast perfusion. Similar to HEK293 cells, rapid glutamate application to patches excised from GluR6 wt induced fast desensitizing responses. However, the same application to patches excised from oocytes expressing the double-cysteine mutant resulted in completely nondesensitizing currents (Figure 2B). Western blot analysis under nonreducing conditions further confirmed the formation of a disulfide bond between the introduced cysteines in R6(K696C/E787C), but not in GluR6 wt or in the single-cysteine mutants (Figure 2C). Taken together, these results support our conclusion that stabilization of the dimer interface leads to desensitization block, as seen for the L-to-Y mutation in AMPA receptors (Stern-Bach et al., 1998; Sun et al., 2002).

The L-to-Y mutation in AMPA receptors does not only block desensitization and slow deactivation (Robert et al., 2001; Stern-Bach et al., 1998; Sun et al., 2002), it also increases agonist apparent affinity (Holm et al., 2005; Stern-Bach et al., 1998). Therefore, we wanted to test whether our double-cysteine mutation also has an effect on agonist apparent affinity. We thus measured EC_{50} values for glutamate and kainate (Figure 2D). For both agonists, R6(K696C/E787C) showed ~15-fold increased apparent affinity as compared to GluR6 wt. A significant shift was also observed for R6(K696R) (5-fold, $p < 0.001$), in which the desensitization rate is 5-fold slower (Figure 1), but not for R6(K696C) (data not shown). Because K696 resides on helix F, which contains residues important for agonist binding and stabilization of the intradomain closed-cleft conformation (Armstrong and Gouaux, 2000; Mayer, 2005; Mayer

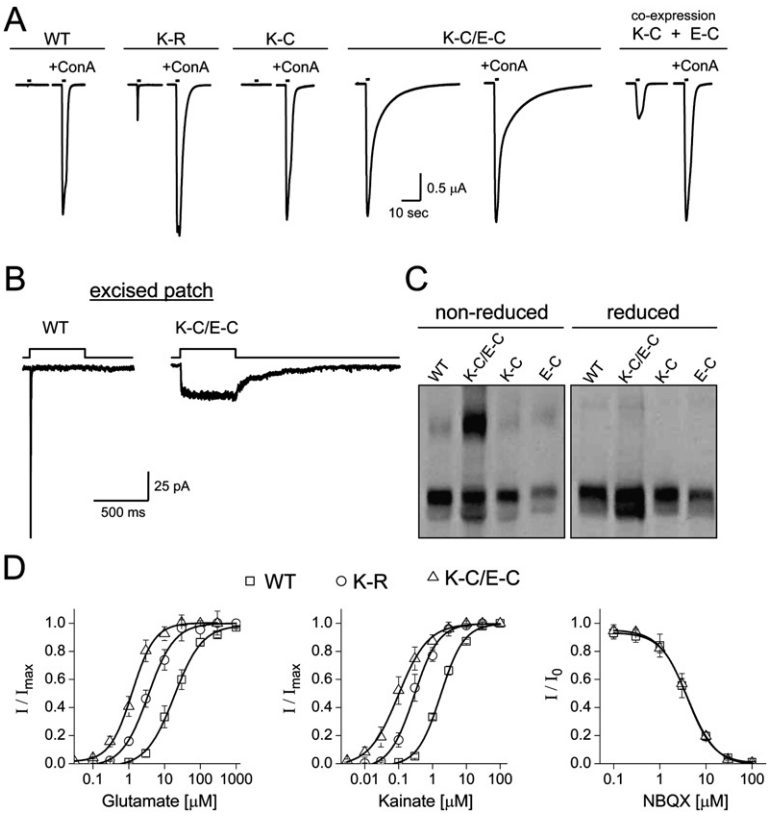

Figure 2. The Double-Cysteine Mutation K696C/E787C Blocks GluR6 Desensitization in *Xenopus* Oocytes

(A) Two electrode voltage-clamp recordings from *Xenopus* oocytes at holding potential of −70 mV. Current traces before and after treatment with the desensitization blocker concanavalin A (+ConA) are shown for the homomeric expression of GluR6 wt, K696R (K-R), K696C (K-C), E787C (E-C), and R6(K696C/E787C) (K-C/E-C), and for the coexpression of K696C and E787C (K-C + E-C). In each case, oocytes were exposed for 2 s to 1 mM glutamate, except for the double-cysteine mutant K-C/E-C, which was exposed to 30 μM glutamate. After 2 min wash, the oocytes were treated with ConA (1 mg/ml) for 5 min, washed for 2 min, and then re-exposed to glutamate for 2 s. The time course of each glutamate application is indicated by a black bar above the corresponding trace.

(B) Recordings from excised outside-out patches pulled from *Xenopus* oocytes expressing GluR6 wt or the double-cysteine mutant (K-C/E-C) demonstrate the lack of receptor desensitization in the mutant on a fast timescale.

(C) Western blot analysis (4%–12% gradient SDS-PAGE) under nonreducing (−DTT) and reducing (+DTT) conditions demonstrates the formation of a disulfide bond across the dimer interface in the K-C/E-C mutant.

(D) Left and middle panels show dose-response measurements for glutamate and kainate, respectively, on GluR6 (wt; square), R6(K696R) (K-R; circle), and R6(K696C/E787C) (K-C/E-C; triangle). Responses to different concentrations of agonist (I) were normalized to the maximum response obtained at 1 mM glutamate and 0.1 mM kainate, respectively, and fitted with Hill equation. Right panel shows dose-inhibition curve for the competitive antagonist NBQX on GluR6 (wt; square) and R6(K696C/E787C) (K-C/E-C; triangle). Responses (I) to different concentrations of NBQX in the presence of either 30 μM glutamate for GluR6 or 2 μM glutamate for R6(K696C/E787C) were normalized to the glutamate response without NBQX (I_0) and fitted with Hill equation. Each point in the different panels is the mean ± SEM of six to eight oocytes. Glutamate EC_{50} values (μM): 18 ± 1 (wt), 3.5 ± 0.3 (K-R), and 1.24 ± 0.07 (K-C/E-C). Kainate EC_{50} values (μM): 1.7 ± 0.1 (wt), 0.32 ± 0.04 (K-R), and 0.11 ± 0.01 (K-C/E-C). NBQX IC_{50} values (μM): 3.9 ± 0.1 (wt) and 3.9 ± 0.2 (K-C/E-C).

et al., 2006; Nanao et al., 2005; Weston et al., 2006a), it was important to determine whether the change in agonist apparent affinity is due to a change in agonist binding affinity or a change in efficacy (i.e., the coupling efficiency between agonist binding and channel opening). To distinguish between these two possibilities, we determined the IC_{50} values of the competitive antagonists NBQX (Figure 2D) and kynurenic acid (data not shown). No change in IC_{50} was observed for either antagonist, implying that the increase in agonist apparent affinity is a result of increased efficacy.

Overall, the phenotype of the double-cysteine mutant in *Xenopus* oocytes, i.e., lack of desensitization, reduced deactivation, and increased efficacy, resembles the phenotype of the L-to-Y mutation in AMPA receptors (Robert et al., 2001; Stern-Bach et al., 1998; Sun et al., 2002) and the behavior of AMPA receptor-positive allosteric modulators (Jin et al., 2005; Partin et al., 1996; Sun et al., 2002), shown to stabilize the dimer interface. Therefore, we can conclude that, like in AMPA receptors, the stability of the dimer interface is a key determinant in kainate receptor gating as well. During revision of the present manuscript, a paper appeared (Zhang et al., 2006) showing results entirely compatible with our interpretation.

Block of GluR6 Desensitization Impairs Receptor Trafficking

The observation that the double-cysteine mutant R6(K696C/E787C) was functional in *Xenopus* oocytes while no currents could be detected in HEK293 cells suggests that cell-surface expression of this mutant in the HEK293 cells may be impaired. Indeed, confocal microscopy imaging on receptors tagged with EGFP at their N-termini revealed that, unlike GluR6 wt, which is targeted to the cell membrane, R6(K696C/E787C) is retained inside the cell, mostly around the nucleus (Figure 3A). To quantify surface expression, we performed ELISA assays using either HA- or EGFP-tagged receptors, and surface expression was determined as the ratio of immunological labeling of nonpermeable and permeable cells. As seen in Figure 3B, surface expression similar to that of GluR6 wt was observed for the active R6(K696R) and R6(K696C), as well as for the apparent inactive R6(E787C). In contrast, surface expression of the double-cysteine mutant R6(K696C/

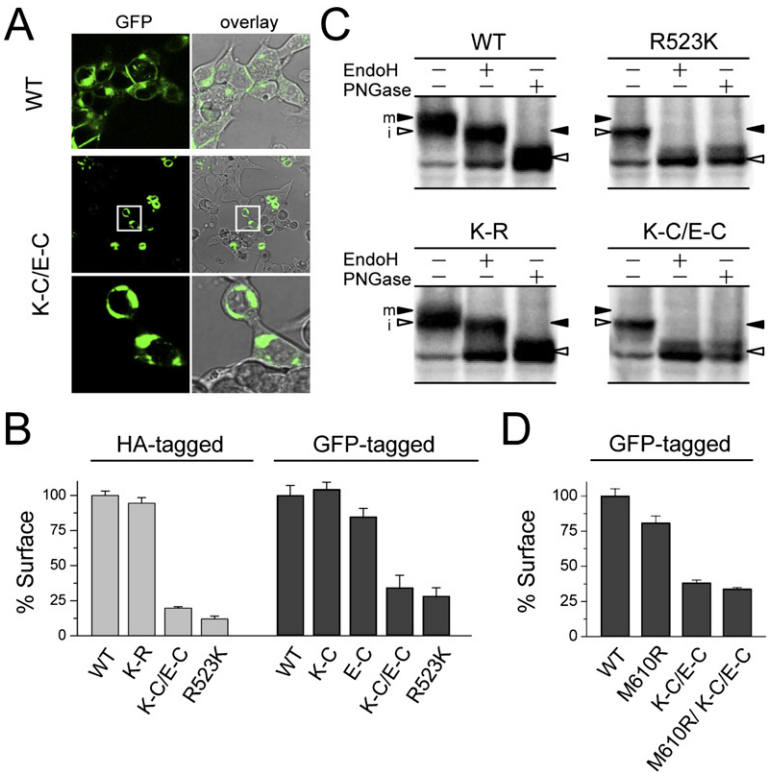

Figure 3. Blocking Desensitization Disrupts Membrane Trafficking of GluR6 in HEK293 Cells

(A) Confocal microscopy imaging of HEK293 cells expressing EGFP-tagged GluR6 wt or the double-cysteine mutant R6(K696C/E787C) (K-C/E-C; the lower panels are inset magnifications). In both cases, pictures represent single confocal sections illustrating GFP fluorescence without (left) and with the transmitted light image (right). Note that while the GluR6 wt is targeted to the cell membrane, the K-C/E-C mutant is sequestered at the ER, giving fluorescence mainly around the nucleus and far from the membrane.

(B) Bar plot of cell-surface ELISA assays done on HEK293 cells expressing HA-tagged (light gray bars) or EGFP-tagged (dark gray bars) constructs. Proteins were detected using HA or EGFP antibodies, and the percentage of surface protein expression (% Surface) was determined as the absorbance ratio of nonpermeable and permeable cells as described in Experimental Procedures. Bars are mean ± SEM of three to four experiments done in duplicate.

(C) Receptor maturation state determined by sensitivity to endoglycosidase H (EndoH). Triton X-100 extracts from HEK293 cells expressing HA-tagged constructs were subject to EndoH treatment to cleave immature glycosylation. The level of fully deglycosylated proteins was determined by treatment with peptide-N-glycosidase F (PNGase). Filled arrowhead denotes maturely glycosylated receptors (m); the empty arrowhead, immature (i). Blots were probed with C-terminal GluR6 antibodies. Shown are representative blots of at least three separate experiments.

(D) Bar plot of cell-surface ELISA on EGFP-tagged constructs performed as described in (B).

E787C) was drastically reduced. Previous studies have shown that mutant kainate receptor subunits incapable of binding glutamate do not traffic to the cell surface (Mah et al., 2005; Valluru et al., 2005). We therefore compared the surface expression of the double-cysteine mutant to that of R6(R523K), a mutant which is both defective in glutamate binding and trafficking (Mah et al., 2005). As seen in Figure 3B, levels of surface expression were similar for both R6(R523K) and R6(K696C/E787C) mutants.

To further examine receptor trafficking, we analyzed the glycosilation state of these mutants by treatment with endoglycosidase H (EndoH) and peptide-N-glycosidase F (PNGase). EndoH specifically cleaves high-mannose-type sugars characteristic of ER resident proteins. High-mannose-type sugars are further processed in the Golgi, and most glycoproteins acquire EndoH resistance. Sensitivity to EndoH therefore reflects the protein maturation state. PNGase, on the other hand, cleaves all N-linked glycans and thus serves as a control for full N-linked deglycosylation. As seen in Figure 3C, the majority of GluR6 wt and R6(K696R) protein is resistant to EndoH (left panels), consistent with the confocal microscopy and the cell-surface ELISA data (Figures 3A and 3B). In contrast, no EndoH-resistant fraction could be observed in R6(K696C/E787C) (bottom right panel) as well as in R6(R523K), which lacks functional glutamate binding (top right panel; Mah et al., 2005). Altogether, these results suggest that the nondesensitizing mutant was retained in the ER. To check that the nondesensitizing receptors are also retained in neurons, we expressed the EGFP-tagged GluR6 wt and R6(K696C/E787C) in cultured hippocampal neurons and included as a control the binding-site mutant R6(R523K). Total protein expression was detected by the GFP fluorescence intensity, and surface expression was determined by exposing the live neurons to anti-GFP antibody. As seen in Figure 4, GluR6 wt was targeted to the membrane, while no surface labeling was observed for either of these two mutants.

It could be argued that the apparent impaired maturation and cell-surface expression of R6(K696C/E787C) may be caused by cell toxicity. Ion flux in response to traces of glutamate in the tissue culture media may cause cell death due to the block of receptor desensitization. This could then result in selection for cells with immature receptors. To test this possibility, we combined the nondesensitizing mutation with a mutation in the channel pore, M610R, shown to impair channel permeation (Robert et al., 2002). Expression of the M610R-containing mutants in *Xenopus* oocytes confirmed the lack of channel activity (data not shown). ELISA assays on HEK293 cells demonstrated that, while R6(M610R) trafficked to the cell surface like GluR6 wt, the triple-mutant R6(M610R/K696C/E787C) did not (Figure 3D). In addition, incubation of cells transfected with R6(K696C/E787C) with the competitive antagonists NBQX or kynurenic acid did not rescue cell-surface expression (data not shown). Finally, no apparent

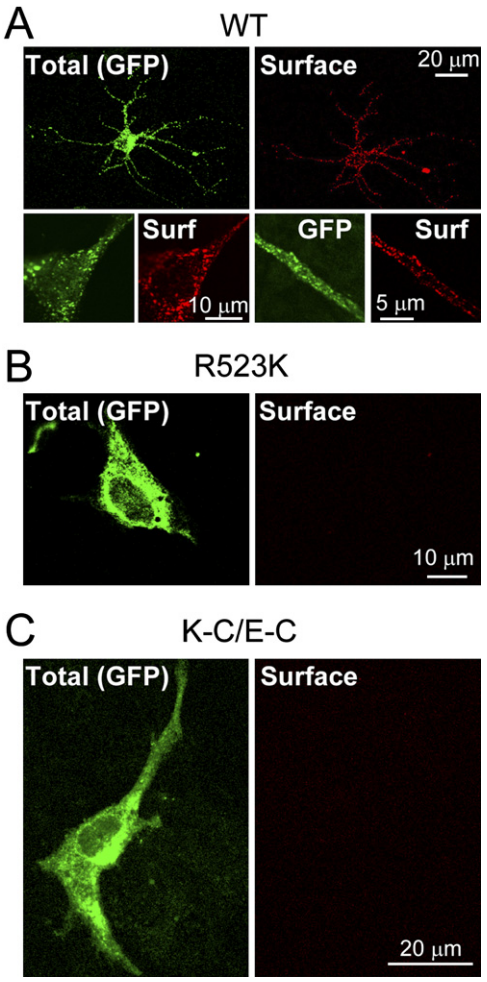

Figure 4. The Nondesensitizing Mutant R6(K696C/E787C) Does Not Traffic to the Membrane in Cultured Hippocampal Neurons

GFP-tagged GluR6 receptors were transfected in cultured hippocampal neurons. Neurons were incubated in vivo with chicken anti-GFP antibody to label receptors present at the surface, followed by Alexa 647-conjugated goat anti-chicken secondary antibody. Panels show total receptor expression visualized as the GFP fluorescence (green), while surface receptors are in red. GluR6 wt (A) traffics to the neuronal membrane. Top panels are average projections of ten confocal sections. The bottom inserts are single confocal sections detailed from separate neurons at the level of neuronal body (left) and a dendrite (right). The binding-site R523K mutant (B) and the nondesensitizing K-C/E-C mutant (C), expressed abundantly (left) but were not detected in the membrane, as judged by the lack of signal in the red channel (right). The examples correspond to a single confocal section taken approximately at the equator of the cell body (B) and an average projection (C).

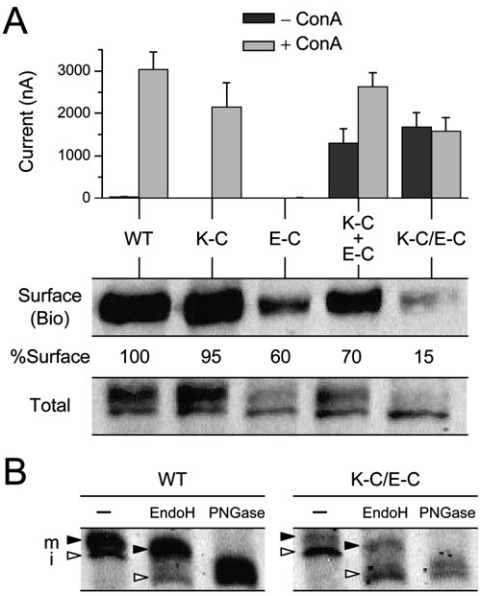

Figure 5. The Double-Cysteine Mutation K696C/E787C Reduces Membrane Trafficking in *Xenopus* Oocytes

(A) Relation between current amplitude and protein surface expression of different constructs expressed in *Xenopus* oocytes. Bar plot shows the mean ± SEM (n = 10 oocytes) of whole-cell currents recorded before (black bars) and after (gray bars) treatment with ConA as described in Figure 2A. Twenty oocytes from the same injection were subjected in parallel to surface biotinylation analysis. Blots of biotinylated (upper panels) and total (lower panels) protein fractions were probed with C-terminal GluR6 antibodies. Bands were quantified with ImageJ; "% surface" reflects the level of biotinylated fraction from the total, normalized to GluR6 wt.

(B) Receptor maturation state measured by EndoH and PNGase digestion on extracts of oocytes expressing GluR6 (wt) or R6(K696C/E787C) (K-C/E-C). Western-blots were probed as described in Figure 3C. Filled arrowhead denotes mature receptors (m); empty arrowhead, immature (i).

differences in the level of cell toxicity could be detected using an in vitro toxicology assay kit based on lactic dehydrogenase (Tox-7, Sigma; data not shown). These results thus exclude cell toxicity as the cause of the apparent impaired trafficking of the nondesensitizing mutant.

The observation that trafficking of the double-cysteine mutant R6(K696C/E787C) in the HEK293 cells was impaired led us to investigate the trafficking in *Xenopus* oocytes, where high activity was observed (Figure 2). Oocytes were injected with GluR6 wt and the various cysteine mutants. Whole-cell current amplitudes and cell-surface expression (measured by cell-surface biotinylation) were determined in parallel. As we observed before, in the presence of ConA, comparable current amplitudes were recorded from GluR6 wt, the single-cysteine mutant R6(K696C) and the double-cysteine mutant R6(K696C/E787C), while no currents were observed for the single-cysteine mutant R6(E787C) (Figure 5A). In contrast, both single-cysteine mutants R6(K696C) and R6(E787C) showed relatively high surface expression (95% and 60%, respectively, measured as the ratio between biotinylated to total protein fraction and normalized to GluR6 wt), while the double-cysteine mutant R6(K696C/E787C) did not (15%). The highly attenuated surface expression of R6(K696C/E787C) was confirmed by the EndoH sensitivity assay (Figure 5B). The relative low surface expression of R6(K696C/E787C), while still retaining high activity comparable to GluR6 wt, is consistent with its increased agonist efficacy (Figure 2D). Taken together, the impaired trafficking of the nondesensitizing mutant in both heterologous cell types and in neurons suggests that the desensitization status of the fully assembled receptor is subject to a quality-control screen in the ER.

To further establish a correlation between block of receptor desensitization and ER retention, we looked

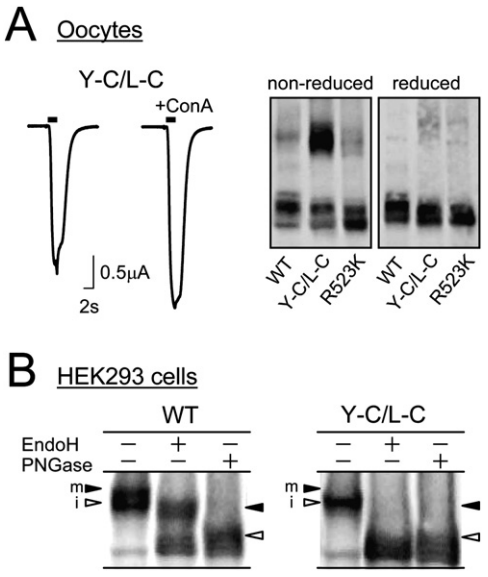

Figure 6. Generation of a Cross-Dimer Disulfide Bond between Residues Y521 and L783 Blocks Receptor Desensitization and Trafficking to the Membrane

(A) Left, whole-cell recordings from oocytes expressing the double-cysteine mutant R6(Y521C/L783C) (see asterisks in Figure 1C), before and after treatment with ConA done as described in Figure 2A; right, Western blot analysis on oocytes' homogenates under reducing and nonreducing conditions shows the formation of a disulfide bond in the double-cysteine mutant Y-C/L-C, but not in GluR6 wt or in the trafficking arrest binding-site mutant R523K.

(B) EndoH-resistant assay on HEK293 cells, done as described in Figure 3C, shows complete lack of receptor maturation of the Y-C/L-C mutant, consistent with lack of surface expression.

for another potential cysteine pair which would generate a cross-dimer disulfide bond. Based on the GluR6 LBD crystal (Mayer, 2005; Nanao et al., 2005), we noticed that Y521, corresponding to the nondesensitizing L-to-Y mutation in AMPARs, is positioned close to L783 of the second monomer (Figure 1C, asterisks). Therefore, we mutated these sites to cysteines. When expressed in *Xenopus* oocytes, this double-cysteine mutant, R6(Y521C/L783C), also exhibited high steady-state currents in response to glutamate, which were only moderately (21% ± 5%, n = 7) increased after treatment with ConA (Figure 6A, left). This is consistent with an apparent block of desensitization due to stabilization of the dimer interface by the formation of a disulfide bond between the introduced cysteines (Figure 6A, right). This mutant was also entirely retained in HEK293 cells as indicated by a complete sensitivity to EndoH deglycosilation (Figure 6B).

The Desensitized Conformation Is a Key Quality Checkpoint for Glutamate Receptor Trafficking

It is now established that in the ER multimeric proteins are subject to a resident quality-control system, which verifies that the proteins are properly folded and assembled before export to Golgi compartments and presentation on the cell surface (Ellgaard and Helenius, 2003; Kleizen and Braakman, 2004; Trombetta and Parodi, 2003). In ionotropic glutamate receptors, subunit assembly masks ER retention signals, especially in heteromeric assemblies that make the majority of native receptors (Isaac et al., 2004; Lerma, 2006; Pinheiro and Mulle, 2006; Vandenberghe and Bredt, 2004). For example, the kainate receptor KA2 subunit contains retention signals in the intracellular C-tail and the loop preceding M3, which prevent ER export unless it assembles with the GluR6 subunit (Nasu-Nishimura et al., 2006; Ren et al., 2003; Yan et al., 2004). Similarly, in AMPA receptors the Q/R site in the pore-forming re-entrant loop is proposed to act as a retention signal that ensures the incorporation of GluR2 R-edited forms in heteromeric assemblies with other AMPA receptor subunits (Greger et al., 2002, 2003).

In addition to proper assembly, recent studies suggest that receptor functionality may also be monitored, because mutations that eliminate glutamate binding in both AMPA and kainate receptor subunits promote retention of these receptors (Grunwald and Kaplan, 2003; Mah et al., 2005; Valluru et al., 2005). Our results with both the K696C/E787C and Y521C/L783C mutations in GluR6, shown to block desensitization and reduce surface expression, demonstrate that the receptor desensitization status is also monitored by the quality-control machinery. This phenomenon is not unique to kainate receptors. Recently, it has been shown that the nondesensitizing L-to-Y mutation in the AMPA receptor GluR2 also leads to ER retention in neurons (Greger et al., 2006). Because these nondesensitizing mutants can bind glutamate, we further suggest that glutamate binding in the ER is needed for the presentation of the desensitized conformation to the quality-control machinery. Moreover, based on the observation that a mutation that blocks ion flow (M610R) not only did not abolish GluR6 trafficking to the cell surface but also did not rescue trafficking of the nondesensitizing receptors (Figure 3D), we also suggest that this quality-control machinery recognizes structural signals in the LBD rather than monitoring channel activity. It is yet to be determined whether this machinery recognizes a specific trafficking motif, exposed or masked at the desensitized state, or monitors the global conformation of the receptor. However, only receptors that achieve the desensitized conformation will be exported to the cell surface (see Figure 7 for illustrative model). Finally, in contrast to the K696C/E787C and Y521C/L783C mutations, surface expression of the R6(K696R) mutant in which desensitization is 5-fold slower (Figure 1) was similar to GluR6 wt (Figures 3). This result, however, does not contradict our model because even though desensitization is significantly slowed, the R6(K696R) mutant is fully converted to the desensitized state due to the continuous presence of glutamate in the ER (Meeker et al., 1989). A similar argument can be provided for the GluR6 interface point mutant K531G (Fleck et al., 2003) and the quadruple mutant R6(K525E/K696R/I780L/Q784K) (Zhang et al., 2006), which although exhibiting slow desensitization, nevertheless undergo desensitization, thus surface expression seems normal. In fact, Greger et al. (2006) showed that the unedited GluR2 at the R/G and flip/flop sites (R-flip), which is less desensitized than the fully edited form (G-flop) assembles and traffics to a greater extent, a phenomenon attributed to a greater stability of the dimer interface in promoting receptor tetramerization (Greger et al., 2006). Due to

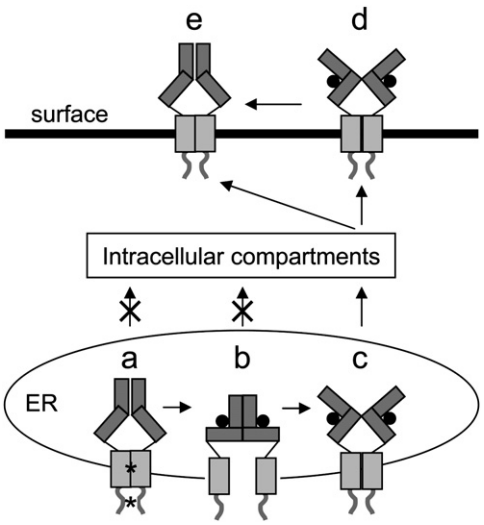

Figure 7. Model of Trafficking Constrains on Glutamate Receptors

The cartoon shows two subunits forming one of the two dimers that assemble an active glutamate receptor. For each subunit, the LBD is shown as two dark gray bars, which correspond to domains 1 and 2. Domain 2 is connected via short linkers (black line) to the channel-forming transmembrane domains, shown as a light gray box. Following is the intracellular CTD drawn as a gray line (the extracellular NTD is omitted). Receptor assembly occurs in the ER (a) and involves masking of retention signals in the CTD and/or the channel domain (marked by asterisks). Glutamate (black circle) binding to the receptor shifts its conformation to the open nondesensitized mode (a to b), which quickly converts to the desensitized state (b to c). Only the latter form is able to traffic to the cell surface (c to d). On the surface, glutamate unbinds (d to e), and the receptor is ready to receive a synaptic input. It is also possible that the unbound-resting conformation is restored in the post-ER secretory compartments (c to e). Receptors unable to bind glutamate, like the R6(R523K) mutant (represented by form a), are arrested and cannot traffic to the next compartment. Receptors that can bind glutamate but cannot desensitize, like the R6(K696C/E787C) mutant (represented by form b), are also trapped. Therefore, glutamate binding in the ER is needed for the presentation of the desensitized conformation to the quality-control machinery.

the highly efficient trafficking of GluR6 wt, we could not determine whether a similar phenomenon occurs with our R6(K696R) mutant.

In conclusion, numerous studies have implicated the activation of both AMPA and kainate receptors in neuronal damage, a process known as glutamate excitotoxicity, which plays a prominent role in both acute (e.g., ischemia) and chronic (e.g., Alzheimer's, ALS, Parkinson's) neurodegenerative disorders (Choi, 1992; Frandsen and Schousboe, 2003; Lerma, 2006; Pinheiro and Mulle, 2006). The fast and profound desensitization of these receptors is thus thought to provide a natural neuroprotective mechanism. Given its importance at the synapse, here we show that the desensitization state is a key checkpoint recognized by the ER quality-control machinery to ensure that only properly working receptors will reach the cell surface.

While this paper was under final review, a paper by Weston et al. (2006b) appeared, which confirms our observation that stabilization of the binding domain dimer interface by disulfide cross-links blocks kainate receptor desensitization.

Experimental Procedures

Molecular Biology

GluR6 (VCQ) was tagged with EGFP at the N-terminus between residues 32 and 33 in pRK5. Amino acid residues are numbered relative to the initiation methionine. Hemaglutinin (HA) tag was inserted at the same place as EGFP using overlap extension PCR. The presence of either tag had no effect on GluR6 kinetics. Point mutations were made using overlap extension PCR and verified by sequencing throughout the amplified cassette. For expression in *Xenopus* oocytes, plasmids were linearized with *Avr II* or *Asp 718* and capped cRNA was transcribed in vitro with SP6 RNA polymerase (mMessage mMachine; Ambion, Austin, TX). The quality of transcripts was assessed by agarose gel electrophoresis and ethidium bromide staining, and the yield was determined using NanoDrop Spectrophotometer (Nanodrop Technology, Wilmington, DE).

HEK293 Cell Culture and Transfection

Human embryo kidney 293 (HEK293) cells were grown in DMEM (Sigma; St. Louis, MO) supplemented with 10% FCS, 100 unit/ml penicillin, 0.1 mg/ml streptomycin, and 1 mM sodium pyruvate (Biological Industries; Beit-Haemek, Israel) at 37°C and 5% CO_2. Cells were passed twice a week until pass #20. Transfections were made using the calcium phosphate method, Polyfect (QIAGEN, Hilden, Germany), or Lipofectamine 2000 (Invitrogen; San Diego, CA). For electrophysiology recordings or confocal microscopy imaging, cells were replated 24 hr after transfection on coverslips coated with poly-D-lysine (0.1 mg/ml; Sigma).

HEK293 Cell Patch-Clamp Recordings

Recordings on HEK293 cells were carried out 36–48 hr after transfection. Membrane currents were recorded at a given membrane potential under the outside-out configuration of the patch-clamp technique using the Axopatch 200B amplifier (Axon Instruments, Foster City, CA) as described previously (Priel et al., 2005). Briefly, membrane currents were digitized online using a Digidata 1322A interface board and pCLAMP 8.2 software (Axon Instruments). Sampling frequency was set to 10 kHz, and the low-pass filter was set to 2 kHz. Patch electrodes were fabricated from borosilicate glass with a resistance of 2–4 MΩ. The extracellular solution contained (mM): 150 NaCl, 2.8 KCl, 0.5 $MgCl_2$, 2 $CaCl_2$, 10 HEPES, adjusted to pH 7.4 with NaOH. The pipette solution contained (mM): 110 CsF, 30 CsCl, 4 NaCl, 0.5 $CaCl_2$, 10 EGTA, 10 HEPES, adjusted to pH 7.2 with CsOH. For the rapid application of glutamate, solutions were applied from a double-barrel glass (theta tube) mounted on a piezoelectric translator (Burleigh, Fishers, NY). We estimated the speed of solution exchange by recording the open tip potentials with solutions of different ionic strengths after expelling the patch from the electrode. The 10%–90% solution exchange was typically <500 μs. Data were analyzed using pCLAMP 8.2 software (Axon Instruments) and Origin 6.1 (Origin Lab Corp., Northampton, MA).

Oocyte Preparation, Electrophysiology, and Western Blot Analysis

Stage V–VI *Xenopus laevis* oocytes were prepared as previously described (Stern-Bach et al., 1994). Oocytes were injected up to 24 hr after isolation with 0.5–5 ng cRNA or 0.2–1 ng cDNA per oocyte, and assayed 1–5 days later. Two electrode voltage-clamp recordings were carried out at room temperature (RT) using GeneClamp500 connected to digidata1322A and pCLAMP8.2 (Axon Instruments). Electrodes (Sutter Instruments, Novato, CA) were filled with 3 M KCl and had resistance of 0.5–1 MΩ. Oocytes were continuously perfused with normal frog ringer (NFR) solution containing (mM): 10 HEPES, pH 7.4, 115 NaCl, 2.5 KCl, 1.8 $CaCl_2$, and 0.1 $MgCl_2$. In experiments where desensitization was blocked, clamped oocytes were incubated with concanavaline A (ConA; Sigma) at 1 mg/ml for 5–10 min before recording. For outside-out patch recordings, the oocytes were incubated for 5–10 min in hypertonic solution (containing in mM: 40 HEPES, pH 7, 60 KCl, 10 EGTA, 8 $MgCl_2$, and 250 sucrose), and the vitelline membrane was removed using forceps. The extracellular solution was NFR, and the pipette solution was as described for the HEK293 cells. Recordings sampling, filtering, and solution exchange were as describe for the HEK293 cells. Data were analyzed using pCLAMP 8.2 and ORIGIN 6.1 software (Origin Lab

Corp., Northampton, MA). Dose-response and dose-inhibition curves were analyzed using ORIGIN 6.1 software (Origin Lab Corp.). For Western-blot analysis under nonreducing conditions, oocytes (10 to 15 per construct) were homogenized with 200 μl lysis buffer containing (mM): 100 NaCl, 100 Tris-Cl, pH 8, 0.5% Triton X-100, and protease inhibitor cocktail (Complete Protease Inhibitors, Roche). The homogenates were incubated on ice for 15 min, centrifuged twice for 10 min at 13000 × g, and the soluble fraction was removed each time to a clean tube. After the second centrifugation, 20 mM NEM was added to the soluble fractions, and centrifugation was repeated twice. Sample buffer containing 63 mM Tris-Cl, pH 6.8, 10% glycerol, 2% SDS, and 0.0025% Bromophenol Blue was added to the homogenate with 50 mM DTT (reduced sample) or without DTT (nonreduced sample). Samples were subject to SDS-PAGE using 4%–12% Tris-glycine gels (Invitrogen) and electroblotted onto nitrocellulose membranes. Blots were incubated with C-terminal anti-GluR6 antibodies (1:2500 dilution; Upstate Biotechnology, Lake Placid, NY) for 1 hr at room temperature, washed, and incubated for additional 1 hr with horseradish peroxidase-conjugated goat anti-rabbit IgG (1:20,000 dilution; Jackson laboratories). Blots were visualized by the chemiluminescence protocol, scanned, and quantified using ImageJ software.

Immunocytochemistry and Surface Labeling of Transfected Neurons

Live cultured hippocampal neurons were prepared using a protocol described elsewhere (Selak et al., 2006). Neurons were transfected at DIV10 with 1 μg of EGFP-tagged GluR6 wt, R6(R523K), or R6(K696C/E787C) using Lipofectamine 2000, according to the manufacturer's instructions. Forty-eight hours later, neurons were washed once with a Ringer buffer containing (mM): 160 NaCl, 15 glucose, 10 HEPES, 2.5 KCl, 1.8 $CaCl_2$, and 1 $MgCl_2$. Neurons were incubated for 1 hr at 16°C with chicken anti-GFP antibody (Aves Labs, Tigard, OR) diluted 1:1000 in the Ringer buffer supplemented with 5% normal goat serum (NGS) and containing 30 μM CNQX and 100 μM D-AP5 to prevent receptor activation. Following the incubation, neurons were washed two times with Ringer buffer and immediately fixed with 4% paraformaldehyde/10% sucrose for 10 min at room temperature. After the fixation step, neurons were washed with PBS and then incubated for 2 hr with Alexa 647-conjugated goat anti-chicken secondary antibody (Molecular Probes/Invitrogen) diluted in PBS containing 2% NGS. Neurons were then washed 2 × 5 min with PBS buffer, mounted onto slides in DAPI-supplemented mounting medium (Vectashield: Vector Laboratories), and viewed using a Leica laser confocal microscope. Similarly, living HEK293 cells, transfected with EGFP-tagged constructs and seeded on coverslips coated with poly-D-lysine, were imaged using a Leica laser confocal microscope equipped with a 63× water-immersion objective.

HEK293 Cell-Surface Enzyme-Linked Immunosorbent Assay

At 24 hr posttransfection, cells from 6-well plates were split to 24-well plates coated with poly-D-lysine (Sigma) and cultured for additional 12–16 hr before analysis. Colorimetric cell-surface ELISAs were performed as described (Ratnam and Teichberg, 2005). Cells were washed once with PBS, fixed for 10 min at RT with 4% paraformaldehyde in PBS, quenched with PBS containing 1% glycine for 10 min, and blocked for 1 hr in PBS containing 4% (w/v) skim milk powder under nonpermeate and permeate (0.2% Triton X-100) conditions. Cells were incubated for 1 hr at RT with primary antibodies (anti-EGFP 1:2000; abcam, Cambridge, UK; or anti-HA 1:500; Roche, Penzberg, Germany), washed three times for 5 min with 4% milk/PBS, and then incubated for 1 hr at RT with the appropriate horseradish peroxidase-conjugated secondary antibodies (Jackson laboratories, West grove, PA) in 4% milk/PBS. The cells were washed with PBS and exposed to o-phenylenediamine substrate (Sigma) in phosphate-citrate buffer, and the color was allowed to develop for 10 min. The reaction was stopped by addition of 0.2 volume of 3 N HCl, and the color intensity was determined with a spectrophotometer at 492 nm.

Surface Protein Biotinylation of *Xenopus* Oocytes

Surface protein biotinylation was done as described previously (Ayalon and Stern-Bach, 2001). Briefly, 20 oocytes expressing the indicated construct were incubated with 0.5 mg/ml EZ-link Sulfo-NHS-SS-Biotin (Pierce, Rockford, IL) in NFR for 30 min at 17°C. Oocytes were washed five times with NFR and homogenized through a p200 pipette tip in Buffer H containing 100 mM NaCl, 20 mM Tris-Cl, pH 7.4, 1% Triton X-100, and protease inhibitor cocktail (Complete Protease Inhibitors, Roche) in a volume of 40 μl per oocyte. Lysates were centrifuged at 14,000 × g for 5 min. Cleared lysate (50 μl) was reserved for whole-cell protein sample (total). The remaining lysate was incubated with 50 μl of 50% streptavidin-Sepharose slurry (Pierce) for 3 hr at 4°C. Beads were washed five times in Buffer H, and biotinylated proteins were eluted by 5 min boiling in SDS-PAGE sample buffer. Total and biotinylated (Bio) fractions were separated on SDS-PAGE (8%), and Western-blot analysis using C-terminal anti-GluR6 antibodies was done as described above.

Deglycosylation with Endoglycosidase H (Endo H) and Peptide-N-Glycosidase F (PNGase)

Total protein extracts from HEK293 cells 36 hr posttransfection were obtained by cell lysis in a buffer containing (mM): 10 HEPES (pH 7.4), 150 NaCl, 1% Triton X-100, and complete protease inhibitor mixture (Roche), followed by centrifugation at 14,000 × g for 15 min to remove the nuclear fraction. Whole-cell extracts from oocytes were obtained as described above. In both cases, 20 μg of total protein were digested with 2 μl of EndoH or PNGase (New England Biolabs) for 2 hr at 37°C following the manufacturer's instructions. Proteins were separated on SDS-PAGE (8%), blotted, and visualized with anti-GluR6 antibodies as described above.

Acknowledgments

This work was supported by grants to Y.S.-B. from the Israel Science Foundation (grant 561/03) and the European Commission (EUSynapse project; contract LSHM-CT-2005-019055) and to J.L. by the Spanish Ministry of Education and Science (grant BFU2006-07138). A.P. is a recipient of the David Kline prize of excellence by the Canadian Friends of the Hebrew University. S.S. is an I3P Program CSIC Research Fellow. We gratefully thank Rocio Rivera for her help with HEK293 cell transfections and Dr. Zehava Siegfried for her help with the manuscript.

Received: August 9, 2006
Revised: November 12, 2006
Accepted: December 4, 2006
Published: December 20, 2006

References

Armstrong, N., and Gouaux, E. (2000). Mechanisms for activation and antagonism of an AMPA-sensitive glutamate receptor: crystal structures of the GluR2 ligand binding core. Neuron *28*, 165–181.

Ayalon, G., and Stern-Bach, Y. (2001). Functional assembly of AMPA and kainate receptors is mediated by several discrete protein-protein interactions. Neuron *31*, 103–113.

Choi, D.W. (1992). Excitotoxic cell death. J. Neurobiol. *23*, 1261–1276.

Dingledine, R., Borges, K., Bowie, D., and Traynelis, S.F. (1999). The glutamate receptor ion channels. Pharmacol. Rev. *51*, 7–61.

Ellgaard, L., and Helenius, A. (2003). Quality control in the endoplasmic reticulum. Nat. Rev. Mol. Cell Biol. *4*, 181–191.

Erreger, K., Chen, P.E., Wyllie, D.J., and Traynelis, S.F. (2004). Glutamate receptor gating. Crit. Rev. Neurobiol. *16*, 187–224.

Fleck, M.W., Cornell, E., and Mah, S.J. (2003). Amino-acid residues involved in glutamate receptor 6 kainate receptor gating and desensitization. J. Neurosci. *23*, 1219–1227.

Frandsen, A., and Schousboe, A. (2003). AMPA receptor-mediated neurotoxicity: role of Ca2+ and desensitization. Neurochem. Res. *28*, 1495–1499.

Greger, I.H., Khatri, L., and Ziff, E.B. (2002). RNA editing at arg607 controls AMPA receptor exit from the endoplasmic reticulum. Neuron *34*, 759–772.

Greger, I.H., Khatri, L., Kong, X., and Ziff, E.B. (2003). AMPA receptor tetramerization is mediated by Q/R editing. Neuron *40*, 763–774.

Greger, I.H., Akamine, P., Khatri, L., and Ziff, E.B. (2006). Developmentally regulated, combinatorial RNA processing modulates AMPA receptor biogenesis. Neuron *51*, 85–97.

Grunwald, M.E., and Kaplan, J.M. (2003). Mutations in the ligand-binding and pore domains control exit of glutamate receptors from the endoplasmic reticulum in C. elegans. Neuropharmacology *45*, 768–776.

Holm, M.M., Naur, P., Vestergaard, B., Geballe, M.T., Gajhede, M., Kastrup, J.S., Traynelis, S.F., and Egebjerg, J. (2005). A binding site tyrosine shapes desensitization kinetics and agonist potency at GluR2. A mutagenic, kinetic, and crystallographic study. J. Biol. Chem. *280*, 35469–35476.

Horning, M.S., and Mayer, M.L. (2004). Regulation of AMPA receptor gating by ligand binding core dimers. Neuron *41*, 379–388.

Isaac, J.T., Mellor, J., Hurtado, D., and Roche, K.W. (2004). Kainate receptor trafficking: physiological roles and molecular mechanisms. Pharmacol. Ther. *104*, 163–172.

Jin, R., Clark, S., Weeks, A.M., Dudman, J.T., Gouaux, E., and Partin, K.M. (2005). Mechanism of positive allosteric modulators acting on AMPA receptors. J. Neurosci. *25*, 9027–9036.

Jones, M.V., and Westbrook, G.L. (1996). The impact of receptor desensitization on fast synaptic transmission. Trends Neurosci. *19*, 96–101.

Kleizen, B., and Braakman, I. (2004). Protein folding and quality control in the endoplasmic reticulum. Curr. Opin. Cell Biol. *16*, 343–349.

Lerma, J. (2006). Kainate receptor physiology. Curr. Opin. Pharmacol. *6*, 89–97.

Madden, D.R. (2002). The structure and function of glutamate receptor ion channels. Nat. Rev. Neurosci. *3*, 91–101.

Mah, S.J., Cornell, E., Mitchell, N.A., and Fleck, M.W. (2005). Glutamate receptor trafficking: endoplasmic reticulum quality control involves ligand binding and receptor function. J. Neurosci. *25*, 2215–2225.

Mayer, M.L. (2005). Crystal structures of the GluR5 and GluR6 ligand binding cores: molecular mechanisms underlying kainate receptor selectivity. Neuron *45*, 539–552.

Mayer, M.L. (2006). Glutamate receptors at atomic resolution. Nature *440*, 456–462.

Mayer, M.L., and Vyklicky, L., Jr. (1989). Concanavalin A selectively reduces desensitization of mammalian neuronal quisqualate receptors. Proc. Natl. Acad. Sci. USA *86*, 1411–1415.

Mayer, M.L., Ghosal, A., Dolman, N.P., and Jane, D.E. (2006). Crystal structures of the kainate receptor GluR5 ligand binding core dimer with novel GluR5-selective antagonists. J. Neurosci. *26*, 2852–2861.

Meeker, R.B., Swanson, D.J., and Hayward, J.N. (1989). Light and electron microscopic localization of glutamate immunoreactivity in the supraoptic nucleus of the rat hypothalamus. Neuroscience *33*, 157–167.

Nanao, M.H., Green, T., Stern-Bach, Y., Heinemann, S.F., and Choe, S. (2005). Structure of the kainate receptor subunit GluR6 agonist-binding domain complexed with domoic acid. Proc. Natl. Acad. Sci. USA *102*, 1708–1713.

Nasu-Nishimura, Y., Hurtado, D., Braud, S., Tang, T.T., Isaac, J.T., and Roche, K.W. (2006). Identification of an endoplasmic reticulum-retention motif in an intracellular loop of the kainate receptor subunit KA2. J. Neurosci. *26*, 7014–7021.

Partin, K.M., Patneau, D.K., Winters, C.A., Mayer, M.L., and Buonanno, A. (1993). Selective modulation of desensitization at AMPA versus kainate receptors by cyclothiazide and concanavalin A. Neuron *11*, 1069–1082.

Partin, K.M., Fleck, M.W., and Mayer, M.L. (1996). AMPA receptor flip/flop mutants affecting deactivation, desensitization, and modulation by cyclothiazide, aniracetam, and thiocyanate. J. Neurosci. *16*, 6634–6647.

Pinheiro, P., and Mulle, C. (2006). Kainate receptors. Cell Tissue Res. *326*, 457–482.

Priel, A., Kolleker, A., Ayalon, G., Gillor, M., Osten, P., and Stern-Bach, Y. (2005). Stargazin reduces desensitization and slows deactivation of the AMPA-type glutamate receptors. J. Neurosci. *25*, 2682–2686.

Ratnam, J., and Teichberg, V.I. (2005). Neurofilament-light increases the cell surface expression of the N-methyl-D-aspartate receptor and prevents its ubiquitination. J. Neurochem. *92*, 878–885.

Ren, Z., Riley, N.J., Garcia, E.P., Sanders, J.M., Swanson, G.T., and Marshall, J. (2003). Multiple trafficking signals regulate kainate receptor KA2 subunit surface expression. J. Neurosci. *23*, 6608–6616.

Robert, A., Irizarry, S.N., Hughes, T.E., and Howe, J.R. (2001). Subunit interactions and AMPA receptor desensitization. J. Neurosci. *21*, 5574–5586.

Robert, A., Hyde, R., Hughes, T.E., and Howe, J.R. (2002). The expression of dominant-negative subunits selectively suppresses neuronal AMPA and kainate receptors. Neuroscience *115*, 1199–1210.

Selak, S., Paternain, A.V., Fritzler, M.J., and Lerma, J. (2006). Human autoantibodies against early endosome antigen-1 enhance excitatory synaptic transmission. Neuroscience *143*, 953–964.

Stern-Bach, Y., Bettler, B., Hartley, M., Sheppard, P.O., O'Hara, P.J., and Heinemann, S.F. (1994). Agonist selectivity of glutamate receptors is specified by two domains structurally related to bacterial amino acid-binding proteins. Neuron *13*, 1345–1357.

Stern-Bach, Y., Russo, S., Neuman, M., and Rosenmund, C. (1998). A point mutation in the glutamate binding site blocks desensitization of AMPA receptors. Neuron *21*, 907–918.

Sun, Y., Olson, R., Horning, M., Armstrong, N., Mayer, M., and Gouaux, E. (2002). Mechanism of glutamate receptor desensitization. Nature *417*, 245–253.

Swanson, G.T., Gereau, R.W., IV, Green, T., and Heinemann, S.F. (1997). Identification of amino acid residues that control functional behavior in GluR5 and GluR6 kainate receptors. Neuron *19*, 913–926.

Trombetta, E.S., and Parodi, A.J. (2003). Quality control and protein folding in the secretory pathway. Annu. Rev. Cell Dev. Biol. *19*, 649–676.

Valluru, L., Xu, J., Zhu, Y., Yan, S., Contractor, A., and Swanson, G.T. (2005). Ligand binding is a critical requirement for plasma membrane expression of heteromeric kainate receptors. J. Biol. Chem. *280*, 6085–6093.

Vandenberghe, W., and Bredt, D.S. (2004). Early events in glutamate receptor trafficking. Curr. Opin. Cell Biol. *16*, 134–139.

Weston, M.C., Gertler, C., Mayer, M.L., and Rosenmund, C. (2006a). Interdomain interactions in AMPA and kainate receptors regulate affinity for glutamate. J. Neurosci. *26*, 7650–7658.

Weston, M.C., Schuck, P., Ghosal, A., Rosenmund, C., and Mayer, M.L. (2006b). Conformational restriction blocks glutamate receptor desensitization. Nat. Struct. Mol. Biol. *13*, 1120–1127.

Yan, S., Sanders, J.M., Xu, J., Zhu, Y., Contractor, A., and Swanson, G.T. (2004). A C-terminal determinant of GluR6 kainate receptor trafficking. J. Neurosci. *24*, 679–691.

Zhang, Y., Nayeem, N., Nanao, M.H., and Green, T. (2006). Interface interactions modulating desensitization of the kainate-selective ionotropic glutamate receptor subunit GluR6. J. Neurosci. *26*, 10033–10042.